

Abstract

The use of computational tools and mathematical modeling has long contributed to our understanding of biochemical networks, in particular, there is a long history of quantitative mechanistic modeling. Currently, there are many existing mathematical approaches to characterize biochemical networks such as cellular metabolism and its regulation. However, many of these methods require detailed kinetic and concentration information that are difficult or even impossible to obtain. In the post-genomics era, large-scale stoichiometric reconstructions of microbial metabolism popularized by static, constraint-based modeling techniques such as flux balance analysis (FBA) have become standard tools. However, FBA models assumes a pseudo-steady-state (QSS) approximation and cannot account for the intracellular dynamics of the the network. Towards those unmet needs, we present a versatile next-generation flux balance analysis model that is capable of capturing intracellular dynamics and concentrations of the network. The access to intracellular information created allowed us to implement preexisting regulatory methods that could not have been done with previous FBA models. The key innovation of our approach is the integration of kinetic-like constraints that works in combination with the objective function to overcome the issues with unidentifiable parameters or mechanisms to predict flux distributions. We tested our approach by modeling dynamic time evolution of two proof-of-concept networks and a *E. coli* central metabolism network. We were able to replicate classically expected gene expression and enzyme kinetic behavior, including diauxic growth phenomenon. While only small-scale networks with simplified gene expression were evaluated, the framework presented here could be an important first step towards modeling large biochemical networks with undetermined mechanisms or parameters, and complex regulation.

Introduction

The use of computational tools and mathematical modeling has long contributed to our understanding of biochemical networks, in particular, there is a long history of quantitative mechanistic modeling [1]. Currently, there are many existing mathematical approaches to characterize biochemical networks such as cellular metabolism and its regulation [2-12]. However, many of these methods require detailed kinetic and concentration information that are difficult or even impossible to obtain. Even with the growing data bases for cellular components and development of new reduced order modeling approaches [13], the applications of many mechanistic modeling methods are limited by the lack of kinetic and concentration information.

To overcome the lack of kinetic information, alternative course-grained modeling approaches have been used to study flux distributions of metabolic networks. In the post-genomics era, large-scale stoichiometric reconstructions of microbial metabolism popularized by static, constraint-based modeling techniques such as flux balance analysis (FBA) have become standard tools [14]. Since the first genome-scale reconstruction of *Escherichia coli* MG1655 by Edwards and Palsson [15], the reconstruction of over 100 organisms followed [16]. The organisms included prokaryotes such as *E. coli* [17] or *B. subtilis* [18] highly sought after in bioprocessing to maximize yields of desired products. More recently network reconstructions have been completed on human as well [19-21]. FBA is a course-grained model that relies on a pseudo-steady-state assumption to reduce unidentifiable kinetic models to an underdetermined linear algebraic system that can be solved efficiently even for large systems. Traditionally, FBA models have lack descriptions of metabolic regulation and control mechanisms that cells need for adapting to different chemical and environmental stimulus. The FBA models instead chooses of pathways in the network by prescribing an objective function on metabolism. The use of an objective function is crucial for FBA models since predictions are highly dependent on the objective function used for the analysis. Common objective functions include maximizing growth [14,22-25], ATP production [26], and the production of desired products [27]. The utilization of objective function is the huge advantage of FBA has over mechanistic models; with little to no kinetic parameters, the maximization of biomass production allows for a wide range of predictions that are consistent with experimental observations for microbial systems [14,22,28-33].

In the last decade, FBA have increased in accuracy and utility by incorporating additional biological knowledge from regulatory constraints, thermodynamics, and alternative classes of objective functions [34]. The second generation FBAs initially approached regulatory constraints as Boolean logic operators [31] that arise based on environmental cues. Palsson and coworkers took a bioinformatics approach and incorporated transcription and translation through the use of the E-Matrix to regulate the metabolism [35]. Meanwhile other second generation FBA models focused on incorporating constraints at a physiological level through the use of crowding constraints, enzyme solubility, or membrane economics that constrains the upper limit on the sum of certain

or all the flux vector to increase accuracy of metabolic models [36-38]. The accuracy of the prediction from constraint-based models such as FBA is heavily based on the constraints implemented to reduced the solution space. The second generation FBAs introduce additional constraints that reshape and reduce the solution space to redirect the flux distribution guided by the objective function in a way that more accurately describe biological behaviors.

In this study, we present an effective biochemical network modeling framework for the construction of next-generation flux balance analysis. The key innovation of our approach is the integration of kinetic-like constraints that works in combination with the objective function to overcome the issues with unidentifiable parameters or mechanisms to predict flux distributions. These kinetic-like constraints are adjustable parameters that are governed by the presence any combination of: substrate, enzyme, and signaling molecules. This integration allows the description of fluxes and complex regulatory interactions such as allosteric regulation of enzyme activity, in the absence of specific kinetic and mechanistic information which limited tradition FBA models. We adopted the regulatory rules and method from [12], which do not rely on overarching theoretical abstractions or restriction assumptions. We tested our approach by modeling the time-evolution of a hypothetical proof-of-concept metabolic network using discretized mass balances. In particular, we verified that our new modeling approach can replicate classically expected gene expression and enzyme kinetic behavior, and additionally, whether we can capture intracellular metabolite concentrations and regulatory behaviors. Towards these questions, we constructed a proof-of-concept metabolic network that have two enzyme-dependent reactions. In the absence of the specific enzymes, the reactions will not occur which the dynamics would not be captured by prior FBA models. We found that our next-generation FBA method has the potential to incorporate gene expression, complex regulatory interactions, and capture intracellular metabolite concentration. Lastly, we tested this framework with a central carbon network for *E. coli* and were able to adjust minimal parameters to fit experimental data of [39] and capture the diauxic effect of carbon utilization. However, with minimal experimental measurements and known parameters, this modeling approach fails to capture intracellular metabolites at an adequate level. However, we believe that this framework presented here could be an important addition to the next-generation FBA models.

Results

1. Formulation of Proof-of-concept Network Model

We developed a proof-of-concept metabolic networks (Figure 1) to investigate the features of our effective biochemical network modeling approach. This ultra-reduced network incorporates metabolic reactions, gene expression, enzyme-dependent reactions, and allosteric regulation. Two examples are presented where extracellular substrate Axt is consumed and utilized in a series of metabolic reactions. Several of these reactions or fluxes involved are enzyme or initiators depended. The fluxes that are

not explicitly enzyme depended assumes that the required enzyme to catalyze the reaction is plentiful and that the flux is only a function of substrate concentration.

The conversion from A to B and extracellular uptake of Cxt is dependent on the presence of enzyme E and C transporter (CT) respectively. The expression of E and CT is regulated at the gene expression level. Gene 1 transcribed mRNA E and translated for enzyme E in the presence of growth factors, while Gene 2 expressed CT in a similar manner at a lower concentration of Axt. In the presence of a growth factor that acts as an inducer, the gene for enzyme E will activated and will facilitate transcription and translation reactions to synthesize enzyme E. Meanwhile, in the presence of Axt, the gene expression of of CT repressed. Once the extracellular A is depleted, the C transporter will be synthesized. In our formulation, Hill-like transfer functions were used to calculate the influence of factor abundance upon target enzyme activity. In this context, factors can be a function of metabolite concentration or flux. The kinetic-like constraints are multiplied by an activity control between 0 and 1.

Gene expression in the proof-of-concept network involved a two-step process: transcription and translation. The course-grained transcription and translation reactions in our network neglected the utilization of NTPs and amino acids. Transcription in the proof-of-concept network is solely determined by the presence of relevant inducer, respective gene, and RNA polymerase concentration, and similarly, the translation reactions were determined by mRNA and ribosome concentration. We assumed the generation of RNA polymerase and ribosome synthesis to be a zeroth order constant while degradation to be a first order rate.

A critical test of our modeling approach was to simulate networks with known behavior. If we cannot reproduce the expected behavior of simple networks, then our effective modeling strategy, and particular rules of constraining fluxes, will not be feasible for large-scale networks. We considered two cases, that had identical initial concentrations and kinetic parameters; the only difference between the cases were the objective functions and gene expression. The first case involved the synthesis of Bxt from Axt, a case analogous to the maximization of a desired product while minimizing any undesired byproducts. The second case we tested included the addition of a biomass template reaction and we explored the diauxic growth phenomenon through a simplified representation of carbon catabolite repression.

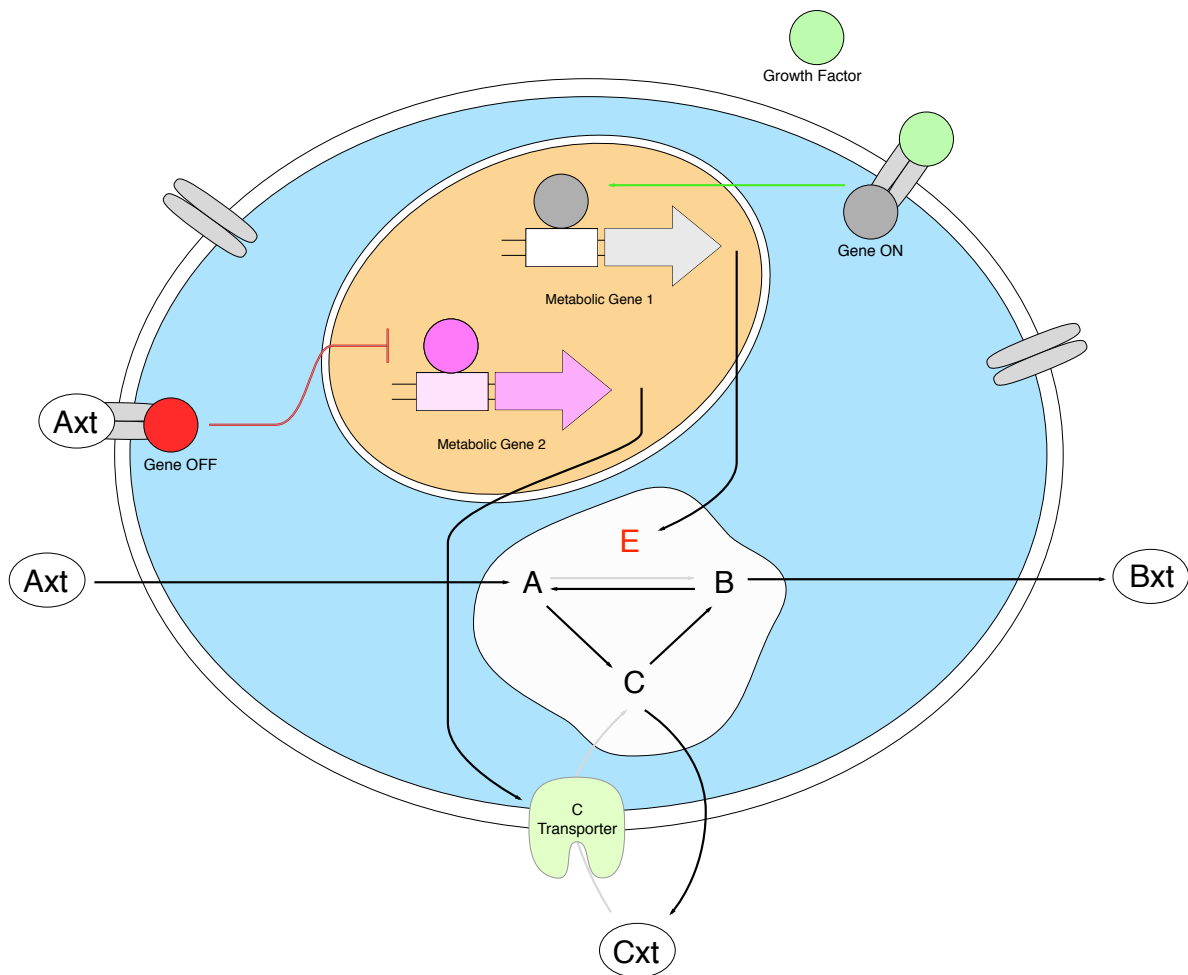


Figure 1. Proof-of-concept metabolic network considered in this study. The black arrows indicate depletion and formation, the red arrows indicate repression, the green represents activation, and the grey arrows are enzyme-dependent reactions. Substrate Axt can be transported into the cell and converted into B and C to be transported out. The reaction that are enzyme dependent are subjected to regulation with respect to gene expression (enzyme E and C transporter).

1.1 Dynamics of inducers and enzyme dependent reactions

The following study focused on the impact of growth factor (inducer) on network aimed at the production of Bxt. Metabolic Gene 2 (Figure 1) responsible for the expression of CT was not included. The growth factor concentration was varied systematically in a linear fashion and the dynamic changes in system was determined. We implemented the objective function to maximize for the production of Bxt. The intracellular metabolites concentrations were constrained at a lower limit of zero while the flux bounds were implemented as a function of substrate concentration, control parameters, and enzyme

concentration for the reactions that are enzyme dependent. The biomass was kept at a constant of 0.1 gDW/L without any growth.

Gene expression of enzyme E was governed by the concentration of the inducer, growth factor. With the increase of inducer concentration, we observed an increase in mRNA and enzyme concentration until steady state as expected (Figure 2A).

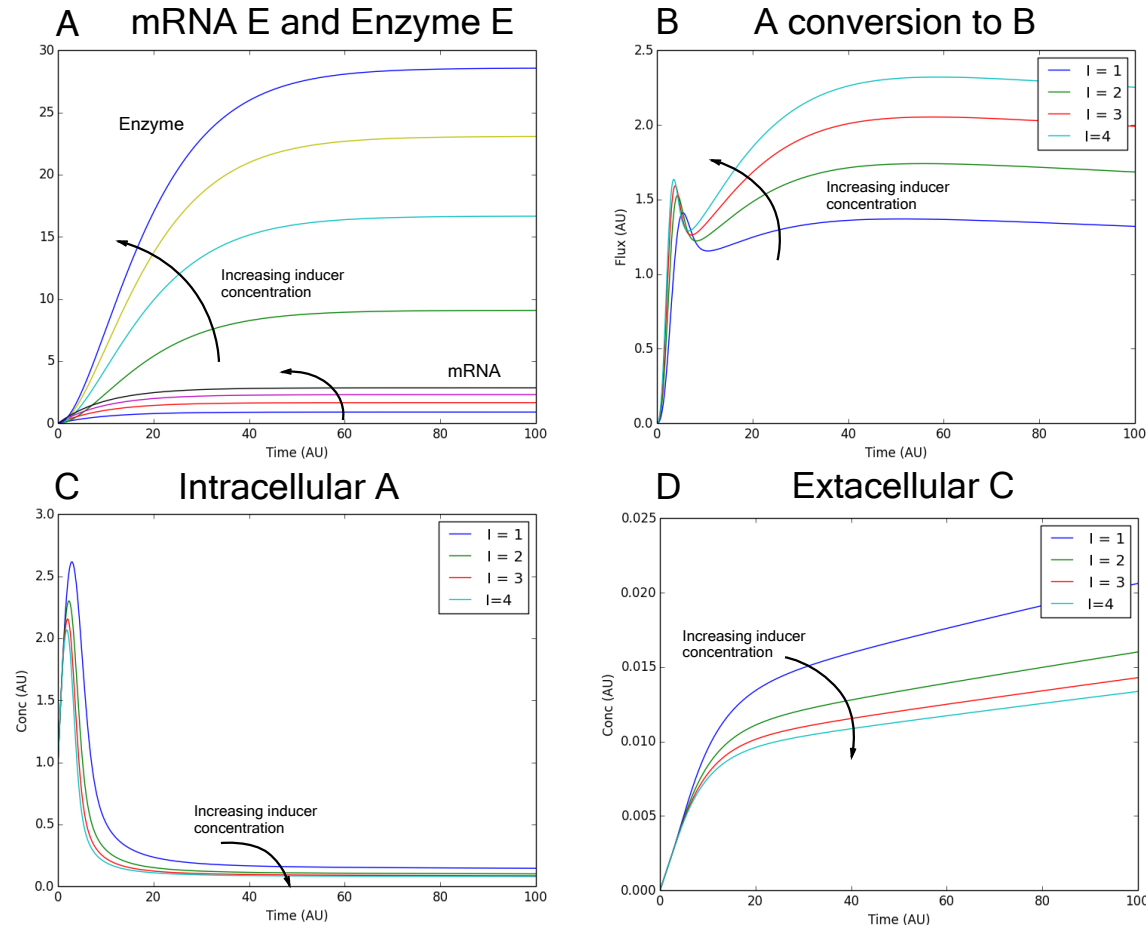


Figure 2. (A) mRNA E and Enzyme E response for different growth factor concentration. Inducer concentration of zero did not express any mRNA or Enzyme (not shown). (B) Flux of A to B catalyzed by Enzyme E. The rate of A conversion to B is proportional to the Enzyme E and substrate A concentration. (C) Intracellular concentration of A. (D) Cxt concentration in the absence of C transporter. The production of Cxt decreases with increasing growth factor inducer concentration.

The presence of Enzyme E facilitated the conversion of A to B. The rate of conversion was governed by the concentration of both of the Enzyme E and species A. The rate of conversion of A to B is shown in Figure 2B. At inducer concentration of zero, the rate of conversion is zero (not shown). Initially, the rate of A_{ext} uptake was greater than the consumption of species A (Figure 2C). As enzyme E accumulated, the conversion of A to B increased proportionally to enzyme E and substrate A concentration. The total rate of

A consumption became greater than the generation, depleting until intracellular A reaches steady state.

The gene expression of enzyme E redirected the pathway of synthesis for product Bxt. In the absence of enzyme E, B can only be formed from the longer path of conversion of A to C to B (Figure 1). This longer path lead to an increased production of undesired by product Cxt (Figure 2D). The presence of Enzyme E opens a new pathway for the direct synthesis of Bxt through the conversion of A to B (Figure 1) and reduce the accumulation of intracellular C and by product Cxt (Figure 2D).

1.2 Dynamics of Growth and Alternative Substrate Utilization

The proof-of-concept network was used to test whether our approach is capable of capturing the diauxic growth phenomenon observed in bacteria using gene expression to regulate the metabolism. A biomass template reaction of intracellular metabolite consumption was constructed:



The growth factor that is responsible for the expression for enzyme E that catalyzes the conversion of A to B was maintained constant at zero. The objective function was implemented to maximize biomass production and the species and flux constraints were implemented the same way as the previous case.

We used an initial biomass concentration of 0.1 gDW/L, and the growth rate constrained to be between 0 and 1, and initiated the simulation with 10 arbitrary units of Axt. The extracellular product, Cxt is generated as a byproduct from the production of all the biomass precursors (Figure 5A) since the presence of species C drives the flux of C to Cxt. As Axt began to deplete, the repression of CT gene expression decreased gradually in a sinusoidal behavior with respect to Axt concentration. When all of the Axt was consumed, gene expression of CT became uninhibited and the production of CT allowed the network to uptake Cxt and utilize it as an alternate substrate for growth (Figure 1 A&B).

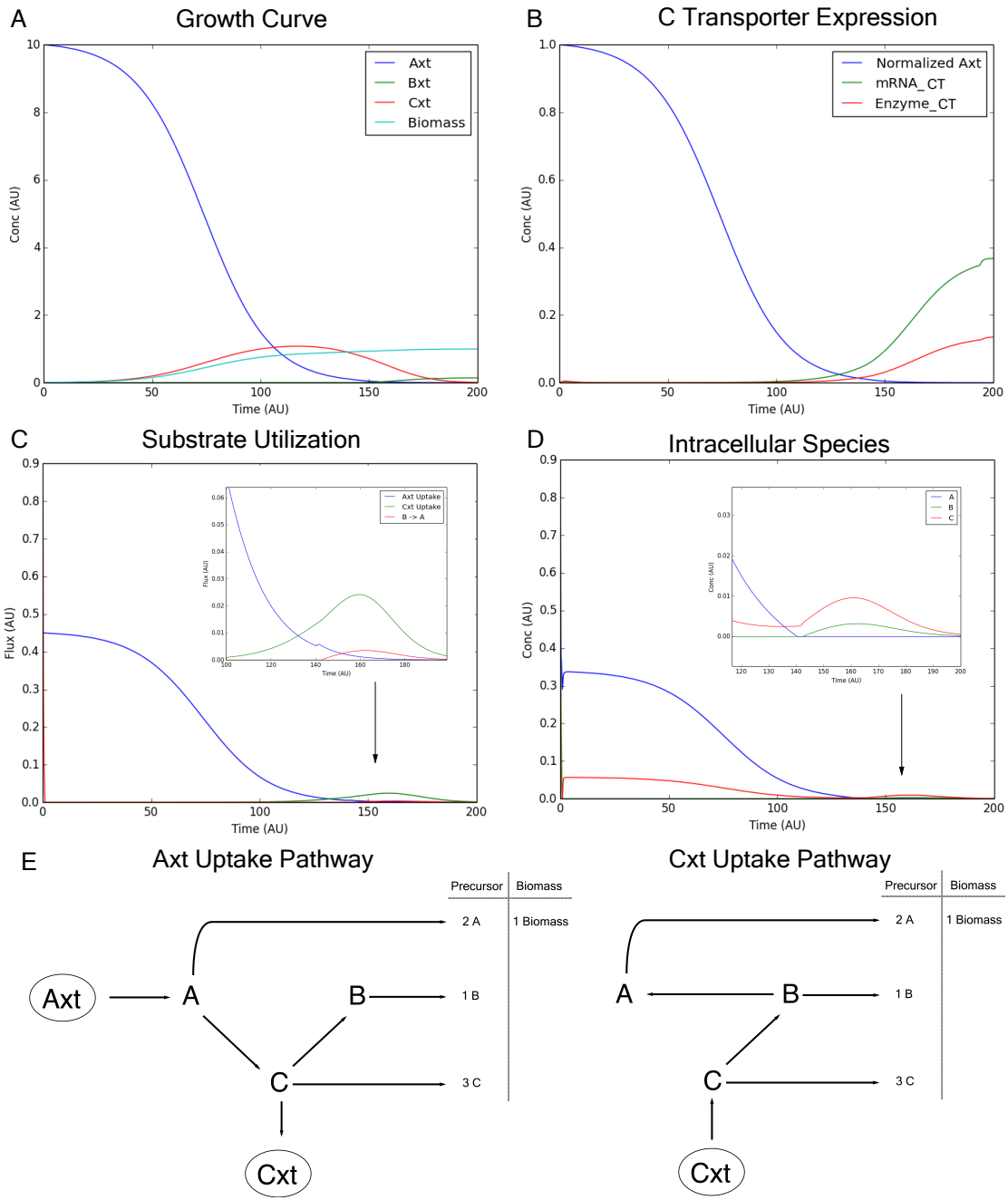


Figure 3. (A) Growth Curve indicates the utilization of Cxt as an alternate substrate when Axt is depleted. (B) Production of mRNA C transporter and C transporter enzyme begins once the Axt concentration is below it's inhibition threshold concentration. (C) The conversion of B to A is required for intracellular replenishment for growth upon Axt depletion. (D) Concentration of intracellular species. (E) Linear pathway of metabolic flux. (A) While Axt is available, intracellular A, C and B are first, second, and third species respectively in the linear pathway. (B) Once Axt is depleted and Cxt is utilized as an alternate substrate, the order of the pathway changes to C, B, and A.

With the proof-of-concept model, we were able to capture the diauxic growth phenomenon with regulation at the gene expression level. We witnessed a decrease in intracellular species concentration due to the decreasing substrate uptake rate relative to the metabolic demand of growth. However, when Axt is depleted, intracellular B and C begins to accumulate due to the relatively high Cxt uptake rate compared to that of Axt uptake rate before complete depletion. As Cxt is consumed, the intracellular concentrations decreased again (Figure 3D).

In addition, we witnessed that the intracellular concentration of B depletes rapidly due to biomass demand (Figure 3D). Species B is synthesized by the conversion from C, and is consumed by the conversion of B to A, biomass synthesis, and dilution due to growth. Intracellular B is the last species in the linear pathway (Figure 3E), the mFBA is optimized to only provide enough B for growth and dilution which kept the B concentration at minimal. Once Axt is depleted, B accumulates and facilitates the conversion of B to A to provide the biomass demand for A. Now A is the last species in the linear pathway, similarly, A concentration becomes minimal. Our method was able to reduce the solution space successfully in capturing complex trends by using simple Hill function and kinetic-like constraints.

1.3 Initialization of *E. coli* Diauxic model

As stated before, a critical test of our modeling approach was to simulate networks with known behavior. We decided to implement our framework on the central carbon metabolism of *E. coli*. In addition, we wanted to test how potential of our modeling approach if the kinetic parameters, mechanistic equations, and regulatory effects within the network architecture was not known. We formed simple regulatory rules based on observation of the experimental data [39] of diauxic growth; that the uptake of acetate was inhibited at high level of glucose uptake. Our *E. coli* model, consists of 65 species and 111 reactions including the template biomass reaction adopted from [41] (Figure 4A). For the initialization of intracellular metabolite concentration, we used measured values from different literature sources [41,42]. For the kinetic-like flux constraints, we decided to implement the classic Michaelis-Menten (MM) kinetics to capture any saturation effects within the system since the metabolite concentration are well above saturation *in vivo* [41].

A critical challenge for any dynamic ODE model is the estimation of kinetic parameters. For metabolic processes, there is also the added challenge of identifying the regulation and control structures that manage metabolism. This issue still exists with this problem, however this challenge can be overcome by increasing the uncertainty of our kinetic-like flux constraints. By doing so, the distance between the upper and lower flux will increase and therefore increasing the solution space and the optimized solution becomes more heavily influenced by the objective function. In our system, we decided to take a coarse-grained approach for parameter estimation to

test the capacity and adaptability of our modeling framework. Using our course-grained parameter estimation approach, the Michaelis Menten parameter were evaluated based on the initial condition of the cellular system. A standard FBA was then carried out, optimizing for growth rate. The calculated solution to the fluxes was then used to evaluate Vmax using initial substrate concentrations and assuming a Km of 1/50 of the species initial concentration. For pathways that were not utilized, ie flux of zero, in the standard FBA solution, the flux constraints were unbound due to the uncertainty. To account for the error and uncertainty associated with this crude estimation, an uncertainty tolerance was placed between the lower and upper bound as a constraint that the flux value must fall within. To determine this variation within the flux constraint, we varied a global parameter across all flux constraints that were govern by MM to fit experimental data. Most of the fluxes in our system were not sensitive to the change solution space. In most metabolic networks, only a few reactions are rate limiting and acts as a bottleneck for the whole system. Increasing the solution space did not impact the fluxes downstream of the bottleneck. This robustness within our system is similar the findings of Sethna and coworkers that model performance is often controlled by only a few parameter combinations, a characteristic seemingly universal for multi-parameter models referred to as sloppiness [43]. Regulatory control was put in place for the uptake of acetate by utilizing a Hill-function govern by the flux of glucose uptake rate of the previous iteration of the discretized mass balance. The parameters in the fill functions were determine by manually fitting against experimental data. The pathways of gluconeogenesis shown in Figure 4A were not regulated, but rather controlled by the optimization from the objective function.

Under the assumed condition, our model was able to accurately capture experimental measurements of extracellular glucose and acetate, and biomass and the glucose-acetate diauxie phenomenon (Figure 4B). However due to the crude parameter estimation, some dynamic resolution of the intracellular concentration were lost. Most of the intracellular metabolites either accumulate or depleted to the concentration limits that were set for the intracellular species. Taking a closer look at two intracellular byproducts of growth, formate and acetate (Figure 4A), both species accumulated towards their respective concentration threshold. However, formate was depleted rapidly until it's lower threshold concentration after it reached the maximum threshold concentration. Upon the depletion of glucose, the state of the system changed to the utilization of acetate leading to a new set of flux distribution. The flux of the glycolysis and gluconeogenesis are shown in Figure 4D. The flux of the glycolysis pathway shown remains constant throughout growth with the utilization of glucose, upon glucose depletion, the flux of gluconeogenesis takes over in supplying carbon into he upper glycolysis and pentose phosphate for biomass precursor production.

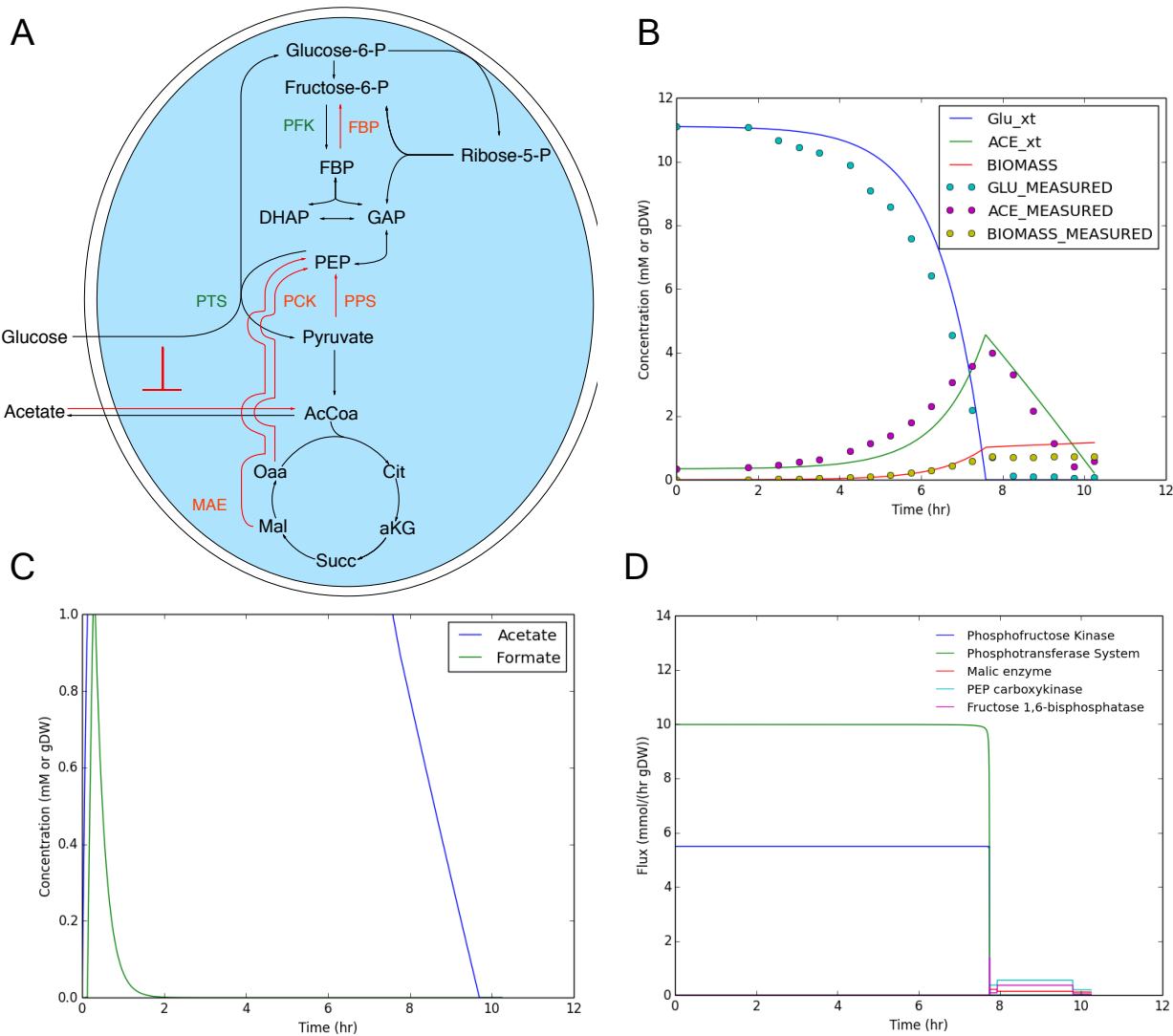


Figure 4. (A) Simplified illustration of the central carbon *E.coli* network. The red arrows represents the fluxes for gluconeogenesis (B) Growth curve showing utilization of acetate compared against experimental measurements from Varma et al 1994. (C) Intracellular metabolite concentration of two by products, acetate and formate. We observed 4 regimes for the intracellular species behavior within this time frame. (D) Flux of glycolysis and gluconeogenesis.

Discussion

In this study, we presented an effective kinetic-like constraint-based FBA model to dynamically simulate metabolic networks. Our proposed strategy integrated kinetic modeling approach with objective function from the traditional FBA to dynamically describe metabolic regulation and control. We tested this model approach by developing a hypothetical proof-of-concept networks and a central carbon *E. coli* network. In

particular, we tested whether our effective modeling approach could describe classically expected behaviors through the combination of regulatory control from allosteric regulation and gene expression. Towards these questions, we explored two hypothetical and one realistic networks. In each of the two hypothetical networks, substrate Axt is transported into the cell and consumed for the production of Bxt or biomass depending on the objective function, while *E. coli* network consumed glucose for the production of biomass precursors for growth. The reactions were assumed to be only substrate-dependent unless specifically implemented to be a function of substrate and enzyme concentrations. Moreover, when these flux constraints were integrated into the network models, these additional constraints captured dynamic patterns in the fluxes and concentration in the network. Lastly, we implemented this method on a central carbon metabolic network of *E. coli*, and captured the diauxic growth phenomenon.

This proposed modeling technique share features with other modeling techniques. The implementation of the flux constraints is flexible and can take the form of most kinetic or mechanistic forms, ie mass action kinetics or effective kinetic formats [44]. Down to the bare bones, this new modeling approach take the form of a discretized form of effective kinetic model in the way that flux constraints that are implemented. The overall purpose of our framework functioned in a similar manner as other FBA models to reduce the solution space to what is biologically or thermodynamically relevant. The real innovation of modeling approach is imploring the use of intracellular metabolite. This subtle difference allowed us to integrate preexisting effective kinetic modeling approaching [12,13] into our kinetic-like constraints. In addition, having access to intracellular species information allowed us to integrate allosteric regulation into the model.

This proposed modeling framework also differs appreciably from previous established FBA models. The vast difference between our proposed method and an ODE models involve the uncertainty that sets tolerance between the governing kinetic form and the upper and lower bound of the flux constraint and the guidance of the objective function. Even with unidentifiable kinetic parameters, this combination high uncertainty and objective function of our modeling approach can overcome this problem. And based on the fluxes that were determined, the kinetic parameters of the most optimized flux distribution can be then determined and analyzed for feasibility. Unlike the previous FBA models, we do not make the quasi-steady-state (QSS) assumption for intracellular species. Our internal species were allowed to accumulate and deplete at a constant rate each time the discretized mass balances were evaluated so that the intracellular concentrations can be captured and implemented as contributors for allosteric regulation. At high uncertainty of the kinetic parameters, we were still able to effectively capture glucose consumption, growth, and the diauxic phenomenon. Unfortunately, dynamic resolution for intracellular metabolites were lost as most the intracellular metabolite approached their upper and lower limits. However, with enough certainty in our parameters, we were able to fully capture the dynamics of intracellular metabolite in our proof-of-concept networks.

In summary, our proposed framework offers an effective method of reducing the solution space of the FBA by using kinetic-like approximations that captured simple enzyme dependence, allosteric regulation, and diauxic growth. At its core, our effective modeling approach combines advantages of FBA and kinetic ODE models. The use of an objective function that acts as a global predictor will overcome problems pertaining unidentifiable parameters or mechanisms, meanwhile the use of kinetic-like constraints on the fluxes acts as a local check-points that reshapes the solution space that is closer to the true behavior of the network. There is a trade off between uncertainty and resolution as expected for any model. At the uncertainty of our system increases, our mFBA approaches the state of a tradition FBA where the solution is determined from the objective function. Meanwhile as uncertainty of our system approaches zero, our modeling approach takes a form that is more similar to an ODE model that is discretized and the solution is shaped by kinetic-like flux constraints. We believe that utilization of this modeling approach is for large networks with unidentifiable parameters or unsalable using ODEs.

Methods

The Modified Flux Balance Analysis (mFBA) is new method created for the study of biochemical networks much like the traditional flux balance analysis. The mFBA utilizes series of species constraints and flux constraints similar to the traditional FBA. The mass balances for each species are discretized and solved using explicit numerical methods such as explicit Euler as in Equations 2 and 3.

$$\frac{dx}{dt} = S * v - \mu x = b \quad (2)$$

$$Intracellular Species: x_{t+1} = x_t + b\Delta t - x_t\mu\Delta t \quad (3a)$$

$$Extracellular Species: x_{t+1} = x_t + b\Delta t\chi \quad (3b)$$

In equation 2, S is the stoichiometric matrix with m species by n reactions, v is a flux vector of each reaction, μ denotes the growth rate and b is a vector of change in species with respect to time. In the discretized mass balances, Equations 3a and 3b, t the time, μ is the growth rate, and χ denotes the species concentration. For traditional FBA, the intracellular species (IS) were assumed to be at quasi-steady-state (QSS), making the species constraint, $b = 0$. However, for the mFBA, we assumed an initial concentration for intracellular species concentration based on literature measurements [41,42] and did not assume QSS by allowing intracellular metabolites to accumulate and deplete within a physiological range. By incorporating the lower and upper limit the species concentration and dilution due to growth, the species constraints implemented in our model is shown in Equation 4.

$$LB - x(1 - dsa * \mu) \leq S * v = b \leq UB - x(1 - dsa * \mu) \quad (4)$$

In Equation 4 LB and UB are vectors of lower and upper limits of each species, while dsa represents the dilution selection array, a Boolean vector that takes determines whether a

species is diluted due to growth, ie. 0 for extracellular species that are not diluted and 1 for intracellular species that are.

The flux constraints use two key components. The kinetics portion are implemented as a function of species concentration in a generalized fashion, and then the regulation portion is incorporated for regulatory mechanisms. The flux is constrained between two a lower and upper bound (Equation 5).

$$\alpha \leq v \leq \beta \quad (5)$$

For tradition FBA, α and β are a vector of constants same length as the number of reactions, for our modeling approach, they are functions of control parameters, substrate concentration, and/or enzyme concentration as shown in Equation 6:

$$\alpha = f_1(\varepsilon)v; \beta = f_2(\varepsilon)v_k \quad (5)$$

where f_1 and f_2 are uncertainty functions of ε , the uncertainty coefficient, a constant that is used to control the solution space in the model based on the certainty in the parameters in the kinetic-like constraints, v_k . The uncertainty functions act as a way to widen the distance between lower and upper limit defined by kinetic-like constraints. The kinetic-like constraints, v_k can take any form, from mechanistic descriptions to effective kinetic models like the power-law:

$$v_k = \alpha x^n * C \quad (6)$$

where α and n represents vectors of gain coefficients and cooperativity coefficients of the power law respectively. The C vector is a control vector that utilizes Hill-functions to describe any types of regulation within the network for both activation and repression.

$$\text{Activation: } C = \frac{\beta x^n}{1 + \beta x^n} \quad \text{Repression: } 1 - \frac{\beta x^n}{1 + \beta x^n} \quad (7)$$

Similarly, β and n represents vectors of gain coefficients and cooperativity coefficients. Lastly, the network is subjected to the objective function, Z :

$$Z = \sum c * v \quad (8)$$

The vector c was used to select a linear combination of metabolic fluxes that were included in the objective function. In our examples, we have defined either production of desired species or cellular growth to be our objective function.

References

1. Bailey, J.E. Mathematical modeling and analysis in biochemical engineering: past accomplishments and future opportunities. *Biotechnol. Prog.* **14**, 8–20 (1998).
2. Castellanos, M.; Wilson, D.B.; Shuler, M.L. A modular minimal cell model: Purine and pyrimidine transport and metabolism. *Proc. Natl. Acad. Sci. USA* **2004**, *101*, 6681–6686.
3. Fell, D. *Understanding the control of metabolism*. (Portland Press, London; 1996).
4. Domach, M.M., Leung, S.K., Cohn, R.E. & Shuler, M.M. Computer model for glucose-limited growth of a single cell of *Escherichia coli* B/r-A. *Biotechnol. Bioeng.* **26**, 203–216 (1984).
5. Palsson, B.O. & Lee, I.D. Model complexity has a significant effect on the numerical value and interpretation of metabolic sensitivity coefficients. *J. Theor. Biol.* **161**, 299–315 (1993).
6. Barkai, N. & Leibler, S. Robustness in simple biochemical networks. *Nature* **387**, 913–917 (1997).
7. Liao, J.C. Modelling and analysis of metabolic pathways. *Curr. Opin. Biotechnol.* **4**, 211–216 (1993).
8. Novak, B. *et al.* Finishing the cell cycle. *J. Theor. Biol.* **199**, 223–233 (1999).
9. Kompala, D.S., Ramkrishna, D., Jansen, N.B. & Tsao, G.T. Investigation of bacterial growth on mixed substrates. Experimental evaluation of cybernetic models. *Biotechnol. Bioeng.* **28**, 1044–1056 (1986).
10. Palsson, B.O., Joshi, A. & Ozturk, S.S. Reducing complexity in metabolic networks: making metabolic meshes manageable. *Fed. Proc.* **46**, 2485–2489 (1987).
11. Conrado RJ, Mansell TJ, Varner J, and MP DeLisa (2007) Stochastic reaction-diffusion simulation of enzyme compartmentalization reveals improved catalytic efficiency for an engineered bacterial propanediol pathway. *Metabolic Engineering*
12. Wayman J, Sagar A and J. Varner (2015) Dynamic Modeling of Cell Free Biochemical Networks using Effective Kinetic Models. *Processes*
13. Sagar A., and Varner J (2015). Dynamic Modeling of the Human Coagulation Cascade Using Reduced Order Effective Kinetic Models. *Processes* **2015**, *3*(1), 178-203
14. Lewis, N.E.; Nagarajan, H.; Palsson, B.O. Constraining the metabolic genotype-phenotype relationship using a phylogeny of in silico methods. *Nat. Rev. Microbiol.* **2012**, *10*, 291–305.

15. Edwards, J.S.; Palsson, B.O. The Escherichia coli MG1655 in silico metabolic genotype: Its definition, characteristics, and capabilities. *Proc. Natl. Acad. Sci. USA* 2000, 97, 5528–5533.
16. Feist, A.M.; Herrgård, M.J.; Thiele, I.; Reed, J.L.; Palsson, B.Ø. Reconstruction of biochemical networks in microorganisms. *Nat. Rev. Microbiol.* 2009, 7, 129–143.
17. Feist, A.M.; Henry, C.S.; Reed, J.L.; Krummenacker, M.; Joyce, A.R.; Karp, P.D.; Broadbelt, L.J.; Hatzimanikatis, V.; Palsson, B.Ø. A genome-scale metabolic reconstruction for Escherichia coli K-12 MG1655 that accounts for 1260 ORFs and thermodynamic information. *Mol. Syst. Biol.* 2007, 3, 121.
18. Oh, Y.K.; Palsson, B.O.; Park, S.M.; Schilling, C.H.; Mahadevan, R. Genome-scale reconstruction of metabolic network in *Bacillus subtilis* based on high-throughput phenotyping and gene essentiality data. *J. Biol. Chem.* 2007, 282, 28791–28799.
19. Duarte NC, Becker SA, Jamshidi N, Thiele I, Mo ML, Vo TD, Srivas R, Palsson BØ: Global reconstruction of the human metabolic network based on genomic and bibliomic data. *Proc Natl Acad Sci USA*. 2007, 104: 1777-1782. 10.1073/pnas.0610772104.
20. Duarte, N.C. *et al.* Global reconstruction of the human metabolic network based on genomic and bibliomic data. *Proc. Natl. Acad. Sci. USA* **104**, 1777–1782 (2007).
21. Ines Thiele, Neil Swainston, Ronan M T Fleming, Andreas Hoppe, Swagatika Sahoo, Maike K Aurich, Hulda Haraldsdottir, Monica L Mo, Ottar Rolfsson, Miranda D Stobbe, Stefan G Thorleifsson, Rasmus Agren, Christian Bölling, Sergio Bordel, Arvind K Chavali, Paul Dobson, Warwick B Dunn, Lukas Endler, David Hala, Michael Hucka, Duncan Hull, Daniel Jameson, Neema Jamshidi, Jon J Jonsson, Nick Juty *et al.* A community-driven global reconstruction of human metabolism. *Nature Biotechnology* 31, 419–425 (2013) doi:10.1038/nbt.2488
22. Mahadevan R, Edwards JS, Doyle FJ: Dynamic flux balance analysis of diauxic growth in *Escherichia coli*. *Biophys J* 2002, 83:1331-1340.
23. Burgard AP, Maranas CD: Optimization-based framework for inferring and testing hypothesized metabolic objective functions. *Biotechnol Bioeng* 2003, 82:670-677.
24. Edwards JS, Ramakrishna R, Palsson BO: Characterizing the metabolic phenotype: a phenotype phase plane analysis. *Biotechnol Bioeng* 2002, 77:27-36.
25. Van Dien SJ, Lidstrom ME: Stoichiometric model for evaluating the metabolic capabilities of the facultative methylotroph *Methylobacterium extorquens* AM1, with application to reconstruction of C-3 and C-4 metabolism. *Biotechnol Bioeng* 2002, 78:296-312.
26. Ramakrishna R, Edwards JS, McCulloch A, Palsson BO: Fluxbalance analysis of mitochondrial energy metabolism: consequences of systemic stoichiometric constraints. *Am J Physiol Regul Integr Comp Physiol* 2001, 280:R695-R704.
27. Varma A, Boesch BW, Palsson BO: Biochemical production capabilities of *Escherichia coli*. *Biotechnol Bioeng* 1993, 42:59-73.

28. Schilling CH, Covert MW, Famili I, Church GM, Edwards JS, Palsson BO: Genome-scale metabolic model of *Helicobacter pylori* 26695. *J Bacteriol* 2002, 184:4582-4593.
29. Edwards JS, Ibarra RU, Palsson BO: In silico predictions of *Escherichia coli* metabolic capabilities are consistent with experimental data. *Nat Biotechnol* 2001, 19:125-130
30. Ibarra RU, Edwards JS, Palsson BO: *Escherichia coli* K-12 undergoes adaptive evolution to achieve in silico predicted optimal growth. *Nature* 2002, 420:186-189.
31. Covert MW, Palsson BO: Transcriptional regulation in constraints-based metabolic models of *Escherichia coli*. *J Biol Chem* 2002, 277:28058-28064.
32. Edwards JS, Palsson BO: Robustness analysis of the *Escherichia coli* metabolic network. *Biotechnol Prog* 2000, 16:927-939
33. Burgard AP, Maranas CD: Optimization-based framework for inferring and testing hypothesized metabolic objective functions. *Biotechnol Bioeng* 2003, 82:670-677.
34. Kauffman KJ, Prakash P, Edwards JS. Advances in flux balance analysis. *Curr Opin Biotechnol*. 2003 Oct;14(5):491-6.
35. Thiele I, Jamshidi N, Fleming RMT, Palsson BØ (2009) Genome-Scale Reconstruction of *Escherichia coli*'s Transcriptional and Translational Machinery: A Knowledge Base, Its Mathematical Formulation, and Its Functional Characterization. *PLoS Comput Biol* 5(3): e1000312. doi:10.1371/journal.pcbi.1000312
36. Beg QK, Vazquez A, Ernst J, de Menezes MA, Bar-Joseph Z, Barabási AL, Oltvai ZN. Intracellular crowding defines the mode and sequence of substrate uptake by *Escherichia coli* and constrains its metabolic activity. *Proc Natl Acad Sci USA*. 2007 Jul 31;104(31):12663-8. Epub 2007 Jul 24.
37. Shlomi T, Benyamin T, Gottlieb E, Sharan R, Ruppin E (2011) Genome-Scale Metabolic Modeling Elucidates the Role of Proliferative Adaptation in Causing the Warburg Effect. *PLoS Comput Biol* 7(3): e1002018. doi:10.1371/journal.pcbi.1002018
38. Zhuang, Kai, Goutham N Vemuri, and Radhakrishnan Mahadevan. "Economics of Membrane Occupancy and Respiro-Fermentation." *Molecular Systems Biology* 7 (2011): 500. PMC. Web. 27 Apr. 2016.
39. Varma A, Palsson BO. Stoichiometric Flux Balance Models Quantitatively Predict Growth and Metabolic By-Product Secretion in Wild-Type *Escherichia coli* W3110. *APPLIED AND ENVIRONMENTAL MICROBIOLOGY*, OCt. 1994, p. 3724-3731.
40. Schuetz, Robert, Lars Kuepfer, and Uwe Sauer. "Systematic Evaluation of Objective Functions for Predicting Intracellular Fluxes in *Escherichia Coli*." *Molecular Systems Biology* 3 (2007): 119. PMC. Web. 3 May 2016.
41. Bennett, Bryson D et al. "Absolute Metabolite Concentrations and Implied Enzyme Active Site Occupancy in *Escherichia Coli*." *Nature chemical biology* 5.8 (2009): 593–599. PMC. Web. 29 Apr. 2016.

42. Heijnen JJ. Impact of thermodynamic principles in systems biology. *Adv Biochem Eng Biotechnol.* 2010;121: 139-62. doi: 10.1007/10_2009_63. p.5/24
43. Machta, B.B.; Chachra, R.; Transtrum, M.K.; Sethna, J.P. Parameter space compression underlies emergent theories and predictive models. *Science* 2013, 342, 604–607.
44. Heijnen, J.J. Approximative kinetic formats used in metabolic network modeling. *Biotechnol Bioeng.* 2005, 91, 534–545